

Article

Experimental Studies on Co-Combustion of Sludge and Wheat Straw

Zeyu Xue , Zhaoping Zhong * and Bo Zhang

Key Laboratory of Energy Thermal Conversion and Control of the Ministry of Education, School of Energy and Environment, Southeast University, Nanjing 210096, Jiangsu, China; jszyxue@163.com (Z.X.); zhangbo8848@yeah.net (B.Z.)

* Correspondence: zzhong@seu.edu.cn; Tel.: +86-025-83794700

Received: 17 January 2019; Accepted: 12 February 2019; Published: 15 February 2019



Abstract: This work presents studies on the co-combustion of sludge and wheat straw (30 wt % sludge + 70 wt % wheat straw). Prior to the combustion experiment, thermogravimetric analysis was performed to investigate the combustion characteristic of the blended fuel. Results indicated that the blended fuel could remedy the defect of each individual component and also promote the combustion. Co-combustion experiments were conducted in a lab-scale vertical tube furnace and the ash samples were analyzed by Inductively Coupled Plasma Optical Emission Spectrometer (ICP-OES), X-ray Diffraction (XRD), and Scanning Electron Microscope (SEM). Thermodynamic calculations were also made to study the interactions that occurred. Addition of sludge could raise the melting point of wheat straw ash and reduce the slagging tendency. Co-combustion also restrained the release of K and transferred it into aluminosilicate and phosphate. Transfer of Pb and Zn in the co-combustion was also studied. The release and leaching toxicity of the two heavy metals in the co-combustion were weakened effectively by wheat straw. $\text{PbCl}_2(\text{g})$ and $\text{ZnCl}_2(\text{g})$ could be captured by K_2SiO_3 in wheat straw ash particles and generate silicates. Interactions that possibly occurred between K, Zn, and Pb components were discussed at the end of the paper.

Keywords: sludge; wheat straw; co-combustion; thermodynamic calculation

1. Introduction

Biomass energy is attracting the world's attention due to its zero CO_2 emissions and considerable production worldwide. Of all the treatments, combustion has the advantages of a simple process, high heat utilization, and capacity reduction rate. However, its popularization was restrained by slagging, fouling, and ash deposit derived from the alkali contained [1]. Alkali metal, especially potassium, was necessary for plant growth and primarily existed in the form of ionic or soluble salts in straw biomass. Mass fraction of K in the raw dried straw accounted for 0.1~5 wt %; it was mobile and easily to transfer [2]. In the biomass combustion, potassium could: (1) release in the form of $\text{KCl}(\text{g})$; (2) react with Si and form low-melting silicates; and (3) combine with S and cause ash deposits [3–5]. Migration of K in biomass combustion requires monitoring and K-inducing problems need to be resolved.

On the other hand, sludge is a byproduct of sewage treatment, extremely complex, and composed of organic fragments, bacteria, colloids, microorganisms, organic, and inorganic matters. Unstable organic matters in the sludge decomposed and reeked odor, meanwhile the heavy metal contained could also leach out and pollute groundwater [6]. However, sludge was rich in P, which mainly comes from the suspended solids in the raw waste water and phosphorus-based flocculants added in the water treatment. The idea of co-combustion of biomass and sludge has been put forward in recent years and some researchers proved that the co-combustion did mitigate the problems related with

alkali metals in the combustion of biomass [7–9]. In particular, Li revealed the mechanism of potassium phosphate formation during the co-combustion of sludge and straw [10].

Apart from P, Al-based flocculants were another component in the water treatment. Mass fraction of Al in the dried sludge accounted for 15~40% and Al_2O_3 was one of the main components of sludge ash [11]. Our previous studies reported that Al in the coal could react with alkali silicates in the biomass–coal co-combustion, which was the primary reaction between the two fuels and could relieve the agglomeration of bed materials in fluidized beds [12,13]. It could be inferred that similar reactions may also take place in the biomass–sludge co-combustion.

However, sludge from municipal sewage plants contained heavy metals including Zn, Pb, Cu, Cr, and Mn [14,15]. In the incineration of sludge, heavy metals could transfer into flue gas and pollute the ecosystem. According to the release ratio, the elements could be divided into easily volatile elements and semi-volatile elements. Their release was also affected by incineration temperature, excess air coefficient, type of reactor, fuel composition, and so on [16]. Considering the relative content and release characteristics, Pb and Zn in the sludge were paid more attention in sludge combustion. Yu and Zhang found that Cl in the fuel could enhance the release of Pb in that evaporation pressure of chlorides was usually larger than oxides [17,18]. However, some researchers also claimed that Cl did not exert a significant effect on Zn release in sludge combustion compared with other heavy metals [19,20]. Guo conducted the co-firing of sludge and biomass and found Zn and Pb appeared to have different migration characteristics and found Pb was inclined to be enriched in fly ash [21]. Several studies also assessed the risk of heavy metals in the sludge ash, confirming the decreasing effect on heavy metal leaching toxicity in co-combustion [22–24]. In recent years, the chemical equilibrium calculation was also used to investigate the existing form of alkali and heavy metals and it was believed that the theoretical conclusion corresponded basically with experimental results [25,26].

Despite the numerous studies concerning the combustion of biomass and sludge before, the mechanisms of co-combustion characteristics and slagging control in the co-combustion remain unclear and require further investigation. In addition, mineral transformation behaviors, especially heavy metal transfer pathways during co-combustion at different combustion stages, should be investigated.

In this paper, characteristics of sludge–wheat straw co-combustion was investigated firstly, and then interactions concerning K, Zn, and Pb were also studied by thermodynamic calculation and experiment in a tube furnace. Samples produced were analyzed by ICP-OES, XRD, and SEM, respectively. Moreover, thermodynamic calculations were applied to discuss the possible reactions of Pb and Zn in the co-firing. Mass fraction of sludge in the co-combustion was set as 30% considering its relatively lower heat value and higher amount of heavy metals, and could be applied to the existing biomass power plants [21,22].

2. Results and Discussion

2.1. TG and DTG Analysis

The TGA tests of wheat straw, sludge, and their mixture were carried out and the TG and DTG curves of the three fuels are given in Figure 1. For combustion of wheat straw, four distinct stages could be divided. In the initial preheating stage below 200 °C, the wheat straw experienced the loss of free/bound water. The second stage occurred around 310 °C, around which the pyrolysis took place, meanwhile the volatile matter separated out and burned rapidly. At about 500 °C the fixed carbon of the wheat straw began to combust. At about 680 °C the residue burned up and some minerals evaporated, causing a slight decrease of weight. After 700 °C the combustion was largely completed.

For combustion of sludge, three stages could be inferred from the DTG curve. At 100 °C the first peak was caused by the loss of water. The second peak at 300 °C and the third peak at 470 °C were the reaction of volatile matter and fixed carbon, respectively. The maximum weight loss rate was much smaller compared with wheat straw (WS). After 600 °C, the two curves both became flat.

In the condition of the blended fuels combustion, three stages would be concluded on the whole. In the dewater process, the two peaks at 100 °C and 200 °C were brought by the two individual components. In the second stage, the peak was also generated by the superposition of the two individual peaks and the value of the maximum weight loss rate was apparently higher than that of the linear superposition by the two individuals. Additionally, the value of the reaction temperature gained by the experiment was lower than the value calculated. In the third stage, the maximum weight loss rate of carbon residue was lower than the predicted value while the temperature was slightly higher. To conclude, co-combustion was not the simple superposition of the two individuals and interaction did take place, actually improving the combustion condition.

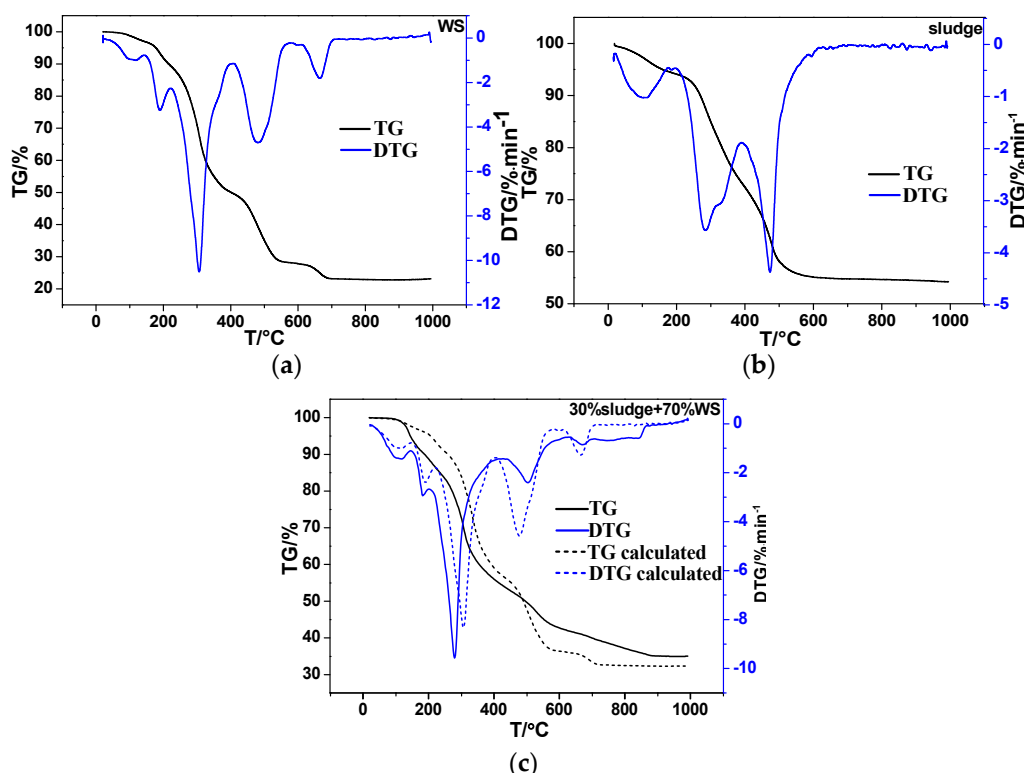


Figure 1. TG and DTG curves of: (a) wheat straw (WS); (b) sludge; (c) 70% WS + 30% sludge in air atmosphere.

2.2. Morphology of Bottom Ash

Figure 2a illustrates SEM micrographs of WS ash at 800 °C. It could be seen that a slight slagging and sintering phenomenon occurred in the surface of WS ash produced at this temperature. Every single submicron particle adhered with each other. However, the morphology of the ash was irregular, and the pore structure was relatively distinct.

WS bottom ash produced at 1000 °C in Figure 2b was found to have the character of experiencing severe liquid-phase melting, the surface was rather smooth and the boundaries between the ash particles became obscure. In addition, the pore structure of the ash almost disappeared and was occupied by eutectic compounds with a low melting point. This could increase the mass transfer resistance and affect the transfer of gaseous species.

In the case of co-combustion at 1000 °C, from Figure 2c it could be inferred that the sludge ash particles appeared in the shape of a group of bricks, of which the size was much larger than WS ash particles. WS ash particles scattered over the surface of the sludge ash. Addition of sludge diluted the ratio of WS ash, thus increasing the gaps between the particles and reducing the tendency of slagging. However, the chemical reaction that occurred also played a role.

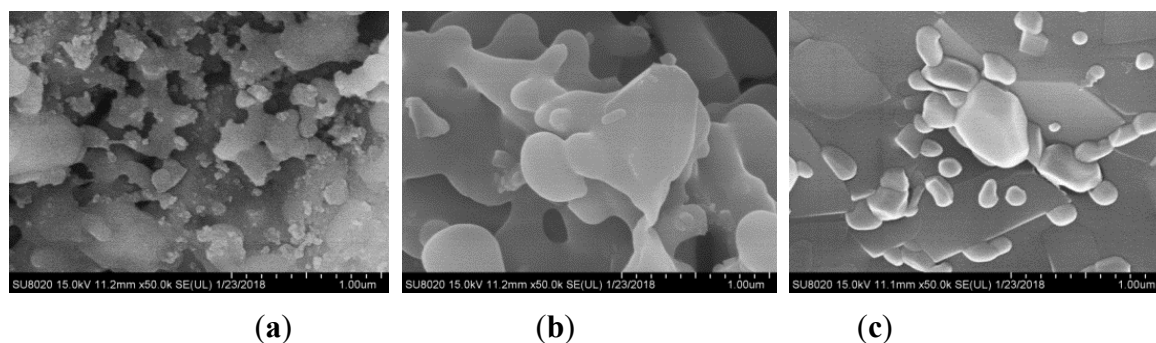


Figure 2. SEM images of ash samples: (a) WS ash produced at 800 °C; (b) WS ash produced at 1000 °C; (c) ash produced in co-combustion at 1000 °C at 50,000 magnification.

To quantify the slagging trend of the ashes, deformation temperature (DT), softening temperature (ST), hemispherical temperature (HT), and flowing temperature (FT) are listed in Table 1.

Table 1. Melting characteristic temperature of the fuel ashes produced at 800 °C. DT: deformation temperature; ST: softening temperature; HT: hemispherical temperature; FT: flowing temperature.

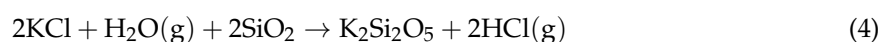
	DT/°C	ST/°C	HT/°C	FT/°C
WS	947	1136	1172	1201
sludge	1195	1289	1310	1324
70% WS + 30% sludge	1021	1194	1221	1243

2.3. Ash Component Analysis

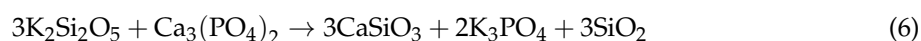
Ash samples were collected and an XRD experiment was conducted. The crystalline phase patterns are shown in Figure 3. For WS ash produced at 600 °C, the crystalline phase detected was KCl, CaSiO₃, SiO₂, and Na₂MgCl₄. Alkali metals mainly existed in the form of chlorides and the peak of Si species was not clear. Sludge ash at 600 °C mainly consisted of SiO₂, KAl₂Si₃AlO₁₀(OH)₂, Fe₂O₃, Al₂SiO₅, and Ca₃(PO₄)₂. In the co-combustion at 600 °C, principal constituents of the ash were SiO₂, KAl₂Si₃AlO₁₀(OH)₂, Fe₂O₃, K₄Ca(PO₄)₂, and 3Al₂O₃·2SiO₂. Potassium chlorides in WS ash could react with Al in the sludge ash and generate muscovite, transforming the soluble, active K into insoluble, stable parts. Additionally, potassium phosphate was also detected. The following reactions may take place in the co-combustion at this temperature.



At 800 °C, WS ash mainly consisted of SiO₂, CaSiO₃, K₂SO₄, and K₂Si₂O₅. It should be noted that potassium chloride totally transferred into other forms. Reactions in Equations (3)–(4) took place with the rise of temperature.



Meanwhile, the chemical composition of sludge ash remained constant during the raising temperature. Blended fuel ash produced at 800 °C consisted of KAlSiO₄, KAlSi₃O₈, SiO₂, Ca₃(PO₄)₂, and K₄Ca(PO₄)₂. Reactions concerning K in the co-combustion at 800 °C are listed below.



When the temperature was enhanced to 1000 °C, the crystallinity became poor due to the melting/sintering that occurred in the WS ash, which was caused by amorphous glassy silicates [12]. The only species detected in the WS ash was SiO₂. Sludge ash at 1000 °C consisted of 3Al₂O₃·2SiO₂, SiO₂, KAlSi₃O₈, Fe₂O₃, Ca₃(PO₄)₂, and Ca₉Fe(PO₄)₇. It could be seen that kaolin was the dominant substance, of which the melting temperature was 1785 °C and was rather stable at high temperatures.

At 1000 °C, ash of the blended fuel was mainly composed of SiO₂, KAlSi₂O₆, KFeSi₃O₈, CaAl₂SiO₆, Ca₇Mg₂P₆O₂₄, and Ca₃(PO₄)₂. K mainly existed in the Al–Si structure and P in the sludge could also react with the K species. Similar results were also found in earlier research [13,27]. The transfer pathway related to K is listed below.



It could be seen that in the co-combustion, K-inducing slagging and melting could mainly be solved by sludge through two mechanisms: (1) Al could react with K and form aluminosilicates in the range of 600~1000 °C; (2) P could react with K and form phosphates at 800 °C. In addition, the reaction degree of K in the WS and sludge was enhanced by the rising temperature. A 30% mass fraction of sludge could also reduce the release of K, Pb and Zn species were not detected due to its relatively low content (<5% in the crystalline phase), which was under the detection limit.

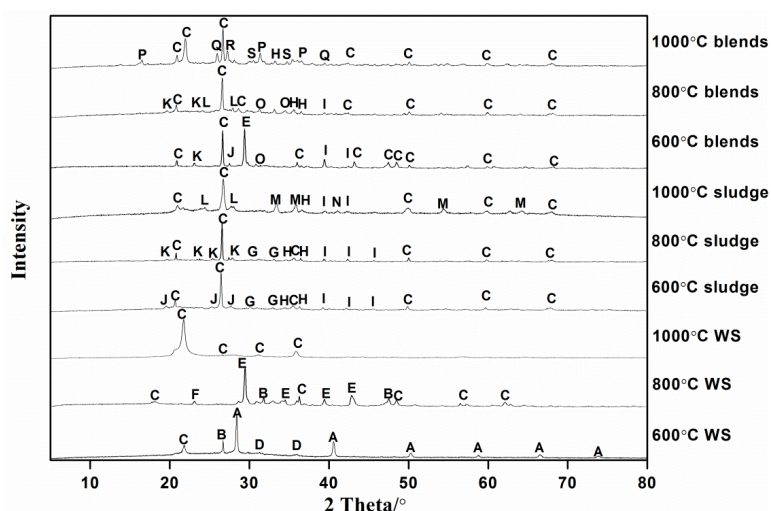


Figure 3. XRD patterns of the ash samples A-KCl, B-CaSiO₃, C-SiO₂, D-Na₂MgCl₄, E-K₂SO₄, F-K₂Si₂O₅, G-Al₂SiO₅, H-Ca₃(PO₄)₂, I-Fe₂O₃, J-KAl₂Si₃AlO₁₀(OH)₂, K-KAlSiO₄, L-KAlSi₃O₈, M-3Al₂O₃·2SiO₂, N-Ca₉Fe(PO₄)₇, O-K₄Ca(PO₄)₂, P-KAlSi₂O₆, Q-KFeSi₃O₈, R-CaAl₂SiO₆, S-Ca₇Mg₂P₆O₂₄.

2.4. K, Pb, and Zn Distribution in the Combustion

2.4.1. Mass Balance Analysis

Figure 4 shows K distribution in the gas phase and bottom ash during the combustion of WS and 70% WS + 30% sludge. In the combustion of WS, release of K was enhanced as the temperature rose up to 900 °C, which could be owing to the improvement in the combustion. At 900 °C, the maximum evaporation rate of 56.6% was reached. In addition, the ratio of soluble K in the ash was reduced, indicating that potassium silicates and aluminosilicates were formed. At 1000 °C, soluble K in the ash only accounted for 5.3%. Compared with the release rate at 900 °C, a decrease at 1000 °C was observed. This phenomenon could be explained by the change in the gas–solid mass transfer coefficient [28]. In the co-combustion, transfer from the soluble K component to the insoluble parts also took place with the increase of temperature, meaning the mobility of K was weakened. For the release of K in the co-combustion, it was smaller than the combustion of WS alone from 600 to 1000 °C. As the temperature was rising, the release ratio initially increased from 600 to 700 °C and it then fluctuated

from 700 to 1000 °C. This was the consequence of the interaction of WS and sludge. In the beginning, the high temperature evaporation dominated the transfer of K before 700 °C. Then the release was relatively restrained due to the intensification of the interaction of K and sludge.

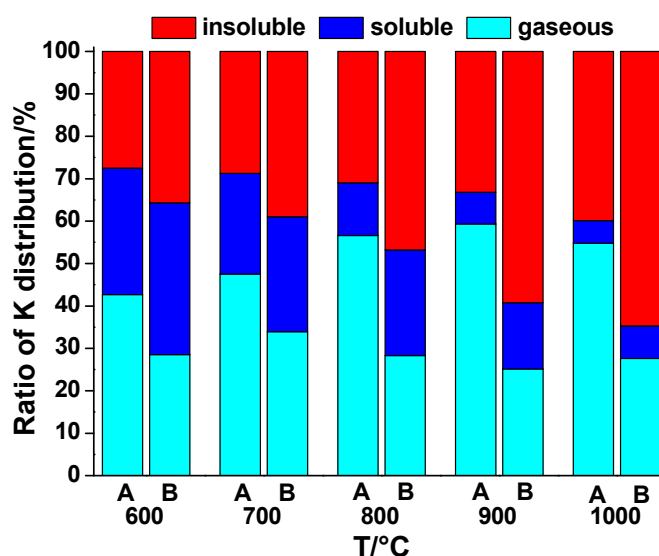


Figure 4. Distribution of K in the case of: (A) WS combustion; (B) co-combustion.

Detailed reactions have been discussed in the former part. To conclude, sludge substituted the element Cl from KCl(g) and released it in the form of HCl(g) instead. The reduction rate of K release by sludge was 33.3%, 28.6%, 50.0%, 57.7%, and 53.4% at 600 °C, 700 °C, 800 °C, 900 °C, and 1000 °C, respectively.

Distribution of Pb and Zn were studied by comparing the co-combustion with sludge combustion. As shown in Figure 5, in combustion of sludge alone, release of Pb was enhanced by the rising temperature in the range 600–800 °C. This was mainly caused by the evaporation of PbCl₂(g), of which the melting point is as low as 501 °C. However, at 900 °C, a clear decrease was observed. This decrease was also substantial in the co-combustion process. This indicated that the released Pb species could be recaptured by other components in the ash while the effect of the evaporation of PbCl₂(g) was relatively impaired.

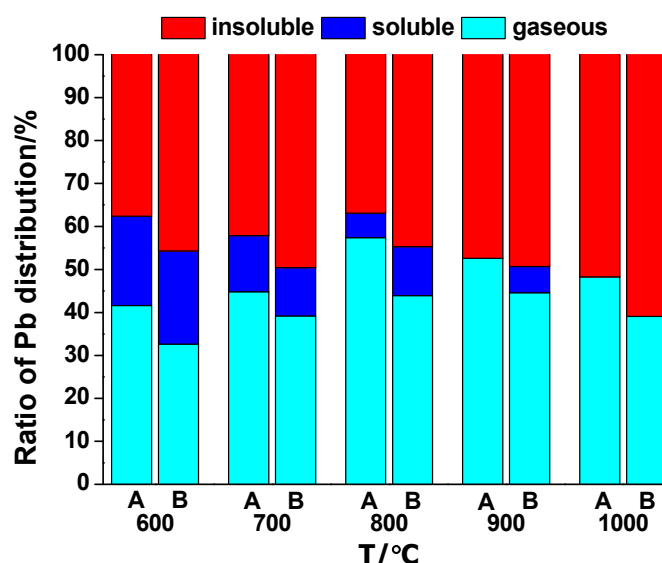


Figure 5. Distribution of Pb in the case of: (A) sludge combustion; (B) co-combustion.

With the presence of wheat straw, the release of Pb was reduced in the co-combustion. As the temperature was rising, the effect of biomass was also augmented. Wang believed that the molten WS ash could also capture released Pb aerosol particles via a physical adhesive force [28]. Meanwhile, share of the soluble Pb component decreased with the temperature; the soluble Pb species was not detected at 900 °C and 1000 °C for sludge combustion and co-combustion, respectively.

For Zn distribution in the sludge combustion, from Figure 6 it was obvious that release of Zn and transfer from the soluble part to the insoluble part were also enhanced by the rising temperature. At 600 °C, the release ratio of Zn was only 25.7% and its maximum value reached 37.1% at 900 °C. The release rate was obviously lower than Pb. The soluble part of Zn in the solid phase reduced from 14.7% to 0% meanwhile. Similar to Pb, co-combustion restrained the release of Zn compared with sludge combustion and the value was in the range of 30.5% to 44.3% and the reducing effect of co-combustion was the most notable at 800 °C. With the temperature rising, the dissimilarity tended to be insubstantial.

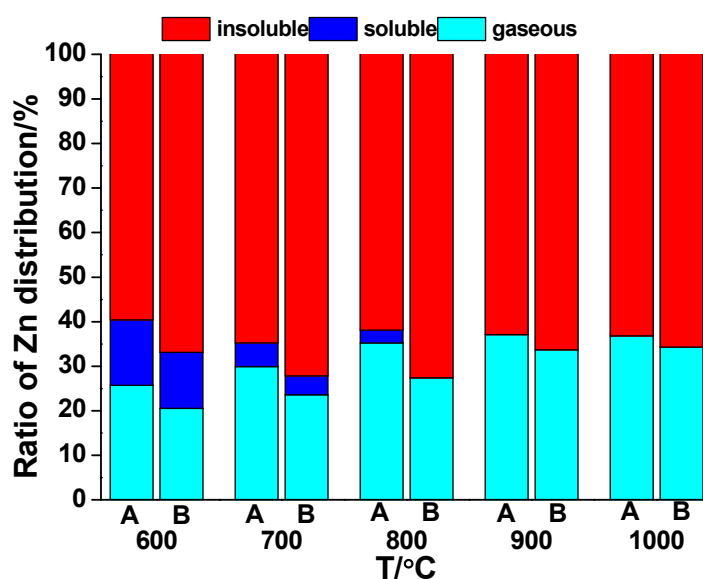


Figure 6. Distribution of Zn in the case of: (A) sludge combustion; (B) co-combustion.

It should be pointed out that co-combustion reduced the soluble part of Zn in the ash and the ratio was below the detection limit since 800 °C. To conclude, the effect of co-combustion on Zn was inferior to Pb due to their different binding capacity to Cl in this temperature range. In addition, high temperature facilitated the combination of potassium silicate and Al in the sludge, thus transferring the silicate into potassium aluminosilicate, increasing the melting point of the bottom ash.

2.4.2. Thermodynamic Calculations on Pb and Zn in the Combustion

Since the relative low content of Pb and Zn in the fuel and their transfer behaviors could not be observed via conventional characterization methods, thermomechanical analysis was applied by the chemical equilibrium calculating tool to further interpret the experiment results. The range of temperature was varied from 550 to 1050 °C and the air-to-fuel ratio was set as 1.2:1 in the calculations. Sludge combustion alone and the co-combustion were calculated respectively.

Figures 7 and 8 indicate the effect of temperature on the transformation of Pb in the sludge combustion and co-combustion, respectively. It could be seen in sludge combustion, Pb mainly existed in the form of PbSiO_3 and $\text{Pb}_3(\text{PO}_4)_2$ at low temperatures, meaning that P and Si in the raw sludge could bind with Pb and restrain its release. As the temperature rose, the phosphate and silicate transferred to $\text{PbO}(\text{g})$, $\text{Pb}(\text{g})$, $\text{PbCl}_2(\text{g})$, and $\text{PbCl}(\text{g})$. Release of the chlorides was enhanced by the rising temperature from 550 to 950 °C. After 1000 °C, $\text{PbO}(\text{g})$ became the dominant Pb-containing species and almost all Pb existed in the gas phase by thermodynamic calculation.

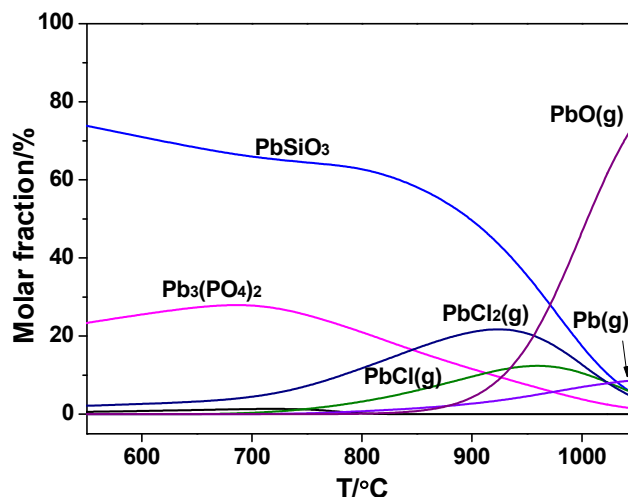


Figure 7. Effect of temperature on the distribution of Pb species in sludge combustion in thermodynamics.

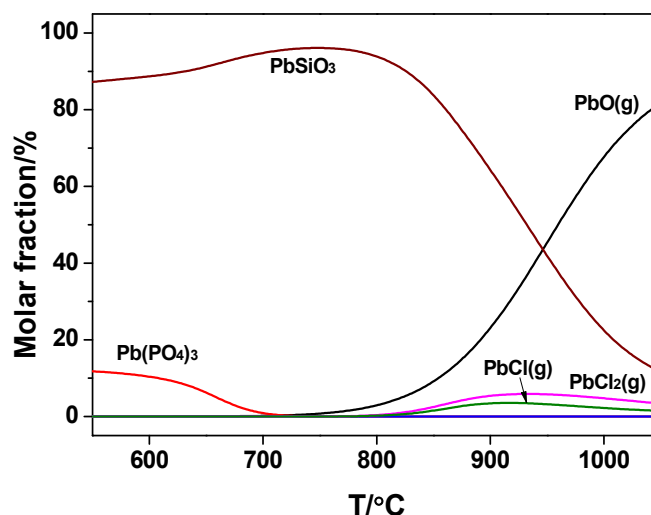
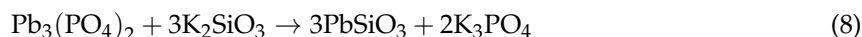


Figure 8. Effect of temperature on the distribution of Pb species in the co-combustion in thermodynamics.

To conclude, the release ratio of Pb in sludge combustion was promoted by the rising temperature, especially after 900 °C due to the decomposition of phosphate and silicate.

However, in the co-combustion, Pb mainly existed in the silicates initially while the content of phosphate was smaller due to the reaction between P and K in the WS via the reaction in Equation (8). This has been discussed in the previous section. Release of chloride was enhanced by temperature in the range 550~920 °C.



Comparing the two cases, it could be inferred that the binding capacity of Cl to Pb was impaired obviously in the co-combustion by calculation. Decrease of Pb release may occur via Equation (9).



As shown in Figure 9, in the combustion of sludge alone, Zn mainly existed in the form of ZnFe_2O_4 and $\text{Zn}_3(\text{PO}_4)_2$ initially. However, the two metal composite oxides decomposed and released free ZnO into the solid phase gradually when the temperature went up. Meanwhile, the release of $\text{ZnCl}_2(\text{g})$ increased slowly as the temperature went up in the range 550~870 °C. By calculation, the

maximum release rate reached 23% at 870 °C and then decreased slowly. Similar results were also gained in previous reports [29].

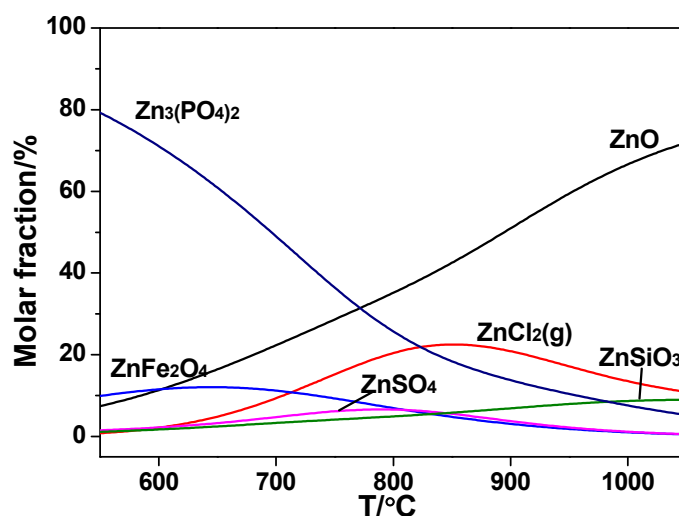


Figure 9. Effect of temperature on the distribution of Zn species in the combustion of sludge in thermodynamics.

In Figure 10, sorts of Zn species are essentially the same, but the relative amounts varied in the co-combustion. Initially the relative content of $Zn_3(PO_4)_2$ was smaller compared with sludge combustion alone, which could be owing to the combination of P and K too.

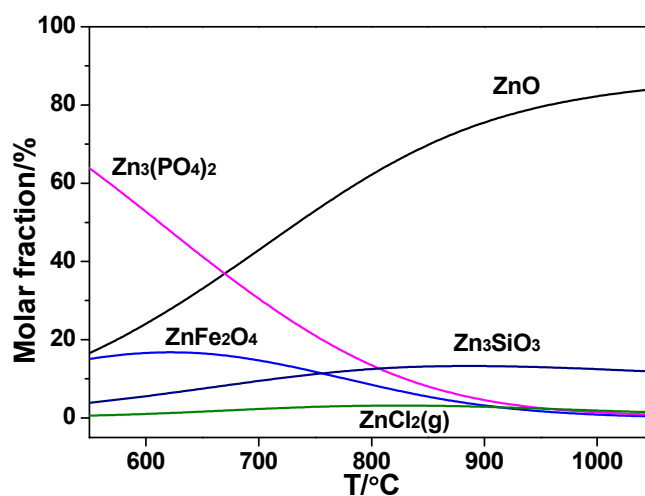
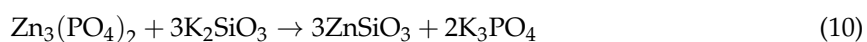


Figure 10. Effect of temperature on the distribution of Zn species in the co-combustion in thermodynamics.

In the range 600~1000 °C, the release rate of Zn was much smaller than sludge combustion due to the decrease in the portion of $ZnCl_2(g)$ by calculation and the relative content only accounted for 4%. Although the value varied widely from the actual release ratio gained by the experiment, it could reveal the decrease of combining capacity of Zn and Cl in the co-combustion. Reactions concerning K and Zn are listed below.



In the WS combustion, Cl primarily occurred in the form of KCl in the solid phase, and in the co-combustion, some share of KCl transferred into HCl(g). Release of the two heavy metals are also affected by Cl, thus there existed a competitive mechanism between K, Pb, and Zn to Cl in the blended fuels. According to the data obtained, possible transfer pathways inferred are shown in Figure 11. The red lines in the figure represent the interactions which took place possibly in the co-combustion.

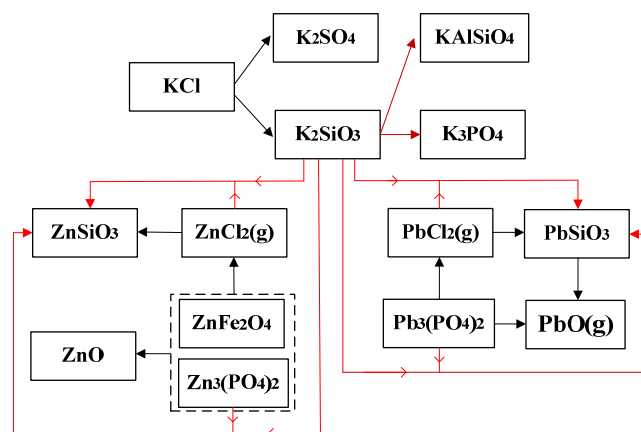
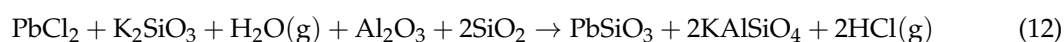


Figure 11. K, Pb, and Zn migration pathways in the combustion.

In the combustion of WS, K mainly existed in chlorides at low temperatures, and with the temperature rising, a portion of KCl evaporated into the gas phase, and the remaining part in the solid phase was inclined to transform into sulfates and silicates, causing the melting phenomena. In the presence of sludge, the incoming Cl was also likely to combine with K, which in the process of release could be recaptured by the Al–Si structure in the sludge ash particles. Wang once reported that the effect of Cl on Pb distribution depended on the content of alkali metals. In the combustion of sludge alone, content of Cl was larger than the sum of K and Na, which indicated that the excess Cl could bond with Pb and Zn at high temperatures [30]. While in the co-combustion, the excess Cl in the sludge, which should have facilitated the release of heavy metals, was inclined to combine with K preferentially. However, the released K then reacted with the Al–Si component in the process of transferring from the inside to the outside of sludge particles. Simultaneously, Zn and Pb were retained in the solid phase, transformed from chlorides to insoluble species. As for Pb, its oxides could combine with Si, however the silicate could decompose at higher temperatures. Likewise, ZnO could also combine with Fe and Al in the combustion. Specially, for Pb, its oxides could also evaporate in the combustion, thus the combination of PbO and SiO₂ determined the release of PbO. The overall reaction at high temperatures could be concluded in Equation (12).



3. Materials and Methods

3.1. Materials

In this study, sludge samples were collected from a local municipal wastewater treatment plant in Nanjing city, Jiangsu province. The wheat straw was collected from Suzhou city, Jiangsu province. The sewage sludge and wheat straw were dried at 105 °C for 24 h and then crushed into particles with the size between 0.10 and 0.15 mm. The dried fuel particles were stored in sample bags for use. Properties of sludge and wheat straw are shown in Table 2.

Table 2. Properties of sludge and wheat straw.

Analyses	Sludge	Wheat Straw
Proximate analysis (wt %, dry basis)		
Ash	55.51	14.80
Volatiles	40.89	64.99
Fixed carbon	3.60	20.21
Ultimate analysis (wt %, dry and ash-free basis)		
C	59.90	51.67
H	7.43	6.21
O	23.28	40.45
N	8.76	1.44
S	0.13	0.53
Main ash forming element (wt %, dry basis)		
Na	0.13	0.05
K	0.07	1.13
Mg	0.23	0.12
Ca	1.96	3.4
Al	11.74	0.25
Si	11.68	2.29
P	1.04	0.21
Fe	1.42	0.17
Cl	0.39	0.35
Heavy metal content (mg·kg ⁻¹ , dry basis)		
Zn	1240.00	45.00
Pb	105.00	13.00

3.2. Experimental Apparatus and Procedure

The thermogravimetric experiment of the fuels was carried out in TGA (SETSYS-1750 CS Evol, SETARAM, Caluire-et-Cuire, France). The fuel samples were heated from room temperature to 1000 °C with the heating rate of 20 °C/min in air atmosphere. The injected sample mass was approximately 6 mg every time.

A horizontal tube furnace was used to investigate the partitioning of potassium and heavy metals and the ash contents in solid residues of wheat straw and sludge during combustion. The quartz tube had an inner diameter of 45 mm and a length of 1000 mm. The combustion air was supplied by an air compressor and the flow rate was set as 0.03 Nm³/h for 45 min. When the temperature reached the value set in advance, about 2 g of wheat straw (WS), sludge powder samples, or their mixture were weighted and mixed evenly in a porcelain combustion boat and pushed into the quartz tube set horizontally in the heating furnace rapidly.

When the combustion was accomplished, bottom ash in the porcelain boat was cooled, collected, and then weighted. Afterwards, the concentration of the digestion solution was analyzed by ICP-OES (Optima8000, Perkin-Elmer, Waltham, USA). The volatilization rate was calculated according to Equations (13)–(16).

$$R = \frac{C_a \times A}{C_{\text{fuel}}} \times 100\% \quad (13)$$

$$V = 100\% - R \quad (14)$$

$$R_s = \frac{C_{\text{as}} \times A}{C_{\text{fuel}}} \times 100\% \quad (15)$$

$$R_{\text{ins}} = R - R_s \quad (16)$$

where C_{fuel} is the initial element concentration in the fuel sample, C_a is the total element concentration in the bottom ash, A is the ash yield, and C_{as} is the soluble element concentration in the bottom

ash. R means the total element retention rate in the bottom ash; R_s and R_{ins} is the water-soluble and insoluble element share in the ash, accordingly.

The crystalline phase of the bottom ash of fuel was determined by X-ray diffraction (SmartLab 3, Rigaku, Tokyo, Japan) over the range 5–90° and the data generated was analyzed by MDI Jade 6.5 (Materials Data Incorporated, Fremont, CA, USA). To analyze the microstructure of bottom ash samples, a scanning electron microscope (SU8010, HITACHI, Tokyo, Japan) was also applied. In addition, the melting point of the ash was analyzed by an ash fusibility tester (SDAF2000D, Sande, Changsha, China) according to GB/219–74.

3.3. Thermodynamic Equilibrium Calculations

To gain information on the transfer of heavy metals in the combustion, thermodynamic equilibrium calculations were also carried out with HSC-chemistry 6.0 software (Outokumpu, Pori, Finland), based on the method of Gibbs free energy minimization. In this paper, the elements C, H, O, N, S, Cl, Si, Al, P, K, Na, Ca, Mg, Fe, Pb, and Zn in the fuels were taken into consideration. The temperature range was between 550 and 1050 °C and the calculated point was set every 25 °C. Air-fuel ratio in the research was set as 1.2:1 and the pressure was 1 bar.

4. Conclusions

Co-combustion experiments at a proportion of 70% WS and 30% sludge were conducted in a TG instrument and a horizontal tube furnace, respectively, to study the combustion characteristics. Results indicated that co-combustion could lower the ignition temperature and increase the combustion quality of sludge. For the blended fuel, the first combustion stage was controlled by wheat straw while the second was mainly affected by sludge.

Sludge could restrain the release of K in the WS combustion effectively and also solve the melting and slagging. Mechanisms could be concluded in two aspects. First, sludge ash separated the WS ash away and reduced the adhesive force between the ash particles. Second, Al and P in the sludge could react with K species and generate high-melting point components. As the temperature rose, the reaction was enhanced.

Transfer of Pb and Zn in the co-combustion was also studied. Similar to K, their release was also restrained in the co-combustion compared with sludge combustion alone. This could be owing to the competition mechanism of Pb/Zn and K on Cl in the blended fuel. K species could substitute Cl from $PbCl_2/ZnCl_2$ and remained the latter in the solid phase. Due to the relative low content of heavy metals in the fuel, the transformation and migration of the trace elements were easily affected by other elements.

Author Contributions: Conceptualization, Z.Z. and Z.X.; methodology, Z.X.; software, Z.X., B.Z.; validation, Z.X., Z.Z. and B.Z.; formal analysis, Z.X.; investigation, Z.X.; resources, Z.Z.; data curation, Z.Z.; writing—original draft preparation, Z.X.; writing—review and editing, Z.Z., B.Z.; visualization, Z.X.; supervision, Z.Z.; project administration, Z.Z.; funding acquisition, Z.Z.

Funding: This research was funded by National Key Research and Development Plan, grant number 2018YFB0605102.

Acknowledgments: This authors wish to acknowledge the financial support provided by the National Key Research and Development Plan (2018YFB0605102).

Conflicts of Interest: The authors declare no conflict of interest.

References

1. Lin, W.; Dam-Johansen, K.; Frandsen, F. Agglomeration in bio-fuel fired fluidized bed combustors. *Chem. Eng. J.* **2003**, *96*, 171–185. [[CrossRef](#)]
2. Khan, A.A.; de Jong, W.; Jansens, P.J.; Spliethoff, H. Biomass combustion in fluidized bed boilers: Potential problems and remedies. *Fuel Process. Technol.* **2009**, *90*, 21–50. [[CrossRef](#)]

3. Nielsen, H.P.; Baxter, L.L.; Sclippab, G.; Morey, C.; Dam-Johansen, K. Deposition of potassium salts on heat transfer surfaces in straw-fired boilers: A pilot-scale study. *Fuel* **2000**, *79*, 131–139. [[CrossRef](#)]
4. Davidsson, K.O.; Åmand, L.; Leckner, B.; Kovacevik, B.; Svane, M.; Hagström, M.; Pettersson, J.B.C.; Pettersson, J.; Asteman, H.; Svensson, J.; et al. Potassium, Chlorine, and Sulfur in Ash, Particles, Deposits, and Corrosion during Wood Combustion in a Circulating Fluidized-Bed Boiler. *Energy Fuel* **2007**, *21*, 71–81. [[CrossRef](#)]
5. Davidsson, K.O.; Åmand, L.E.; Steenari, B.M.; Elled, A.L.; Eskilsson, D.; Leckner, B. Countermeasures against alkali-related problems during combustion of biomass in a circulating fluidized bed boiler. *Chem. Eng. Sci.* **2008**, *63*, 5314–5329. [[CrossRef](#)]
6. Zha, J.; Huang, Y.; Xia, W.; Xia, Z.; Liu, C.; Dong, L.; Liu, L. Effect of mineral reaction between calcium and aluminosilicate on heavy metal behavior during sludge incineration. *Fuel* **2018**, *229*, 241–247. [[CrossRef](#)]
7. Chen, W.; Chang, F.; Shen, Y.; Tsai, M. The characteristics of organic sludge/sawdust derived fuel. *Bioresour. Technol.* **2011**, *102*, 5406–5410. [[CrossRef](#)] [[PubMed](#)]
8. Degereji, M.U.; Gubba, S.R.; Ingham, D.B.; Ma, L.; Pourkashanian, M.; Williams, A.; Williamson, J. Predicting the slagging potential of co-fired coal with sewage sludge and wood biomass. *Fuel* **2013**, *108*, 550–556. [[CrossRef](#)]
9. Aho, M.; Yrjas, P.; Taipale, R.; Hupa, M.; Silvennoinen, J. Reduction of superheater corrosion by co-firing risky biomass with sewage sludge. *Fuel* **2010**, *89*, 2376–2386. [[CrossRef](#)]
10. Wang, X.; Ren, Q.; Li, L.; Li, S.; Lu, Q. TG–MS analysis of nitrogen transformation during combustion of biomass with municipal sewage sludge. *J. Therm. Anal. Calorim.* **2016**, *123*, 2061–2068. [[CrossRef](#)]
11. Parsons, S.A.; Daniels, S.J. The Use of Recovered Coagulants in Wastewater Treatment. *Environ. Technol.* **1999**, *20*, 979–986. [[CrossRef](#)]
12. Zhang, B.; Zhong, Z.; Xue, Z.; Xue, J.; Xu, Y. Release and transformation of potassium in co-combustion of coal and wheat straw in a BFB reactor. *Appl. Therm. Eng.* **2018**, *144*, 1010–1016. [[CrossRef](#)]
13. Xue, Z.; Zhong, Z.; Zhang, B.; Zhang, J.; Xie, X. Potassium transfer characteristics during co-combustion of rice straw and coal. *Appl. Therm. Eng.* **2017**, *124*, 1418–1424. [[CrossRef](#)]
14. Marani, D.; Braguglia, C.M.; Mininni, G.; Maccioni, F. Behaviour of Cd, Cr, Mn, Ni, Pb, and Zn in sewage sludge incineration by fluidised bed furnace. *Waste Manag.* **2003**, *23*, 117–124. [[CrossRef](#)]
15. Liu, J.; Fu, J.; Ning, X.; Sun, S.; Wang, Y.; Xie, W.; Huang, S.; Zhong, S. An experimental and thermodynamic equilibrium investigation of the Pb, Zn, Cr, Cu, Mn and Ni partitioning during sewage sludge incineration. *J. Environ. Sci.* **2015**, *35*, 43–54. [[CrossRef](#)] [[PubMed](#)]
16. Ogada, T.; Werther, J. Combustion characteristics of wet sludge in a fluidized bed: Release and combustion of the volatiles. *Fuel* **1995**, *75*, 617–626. [[CrossRef](#)]
17. Yu, S.; Zhang, B.; Wei, J.; Zhang, T.; Yu, Q.; Zhang, W. Effects of chlorine on the volatilization of heavy metals during the co-combustion of sewage sludge. *Waste Manag.* **2017**, *62*, 204–210. [[CrossRef](#)]
18. Zhang, B.; Bogush, A.; Wei, J.; Xu, W.; Zeng, Z.; Zhang, T.; Yu, Q.; Stegemann, J. Influence of Chlorine on the Fate of Pb and Cu during Clinkerization. *Energy Fuel* **2018**, *32*, 7718–7726. [[CrossRef](#)]
19. Van de Velden, M.; Dewil, R.; Baeyens, J.; Josson, L.; Lanssens, P. The distribution of heavy metals during fluidized bed combustion of sludge (FBSC). *J. Hazard. Mater.* **2008**, *151*, 96–102. [[CrossRef](#)]
20. Cenni, R.; Frandsen, F.; Gerhardt, T.; Spliethoff, H.; Hein, K.R.G. Study on trace metal partitioning in pulverized combustion of bituminous coal and dry sewage sludge. *Waste Manag.* **1998**, *18*, 433–444. [[CrossRef](#)]
21. Guo, F.; Zhong, Z.; Xue, H. Partition of Zn, Cd, and Pb during co-combustion of sedum plumbizincicola and sewage sludge. *Chemosphere* **2018**, *197*, 50–56. [[CrossRef](#)] [[PubMed](#)]
22. Wang, T.; Xue, Y.; Zhou, M.; Yuan, Y.; Zhao, S.; Tan, G.; Zhou, X.; Geng, J.; Wu, S.; Hou, H. Comparative study on the mobility and speciation of heavy metals in ashes from co-combustion of sewage sludge/dredged sludge and rice husk. *Chemosphere* **2017**, *169*, 162–170. [[CrossRef](#)] [[PubMed](#)]
23. Åmand, L.E.; Leckner, B. Metal emissions from co-combustion of sewage sludge and coal/wood in fluidized bed. *Fuel* **2004**, *83*, 1803–1821. [[CrossRef](#)]
24. Zhang, S.; Jiang, X.; Liu, B.; Lv, G.; Jin, Y.; Yan, J. Co-combustion of Bituminous Coal and Pickling Sludge in a Drop-Tube Furnace: Thermodynamic Study and Experimental Data on the Distribution of Cr, Ni, Mn, As, Cu, Sb, Pb, Cd, Zn, and Sn. *Energy Fuel* **2017**, *31*, 3019–3028. [[CrossRef](#)]

25. Sun, Y.; Chen, J.; Zhang, Z. Distributional and compositional insight into the polluting materials during sludge combustion: Roles of ash. *Fuel* **2018**, *220*, 318–329. [[CrossRef](#)]
26. Contreras, M.L.; Arostegui, J.M.; Armesto, L. Arsenic interactions during co-combustion processes based on thermodynamic equilibrium calculations. *Fuel* **2009**, *88*, 539–546. [[CrossRef](#)]
27. Fryda, L.; Sobrino, C.; Cieplik, M.; van de Kamp, W.L. Study on ash deposition under oxyfuel combustion of coal/biomass blends. *Fuel* **2010**, *89*, 1889–1902. [[CrossRef](#)]
28. Wang, X.; Huang, Y.; Zhong, Z.; Yan, Y.; Niu, M.; Wang, Y. Control of inhalable particulate lead emission from incinerator using kaolin in two addition modes. *Fuel Process. Technol.* **2014**, *119*, 228–235. [[CrossRef](#)]
29. Mason, P.E.; Darvell, L.I.; Jones, J.M.; Williams, A. Observations on the release of gas-phase potassium during the combustion of single particles of biomass. *Fuel* **2016**, *182*, 110–117. [[CrossRef](#)]
30. Wang, X.; Huang, Y.; Niu, M.; Wang, Y.; Liu, C. Effect of multi-factors interaction on trace lead equilibrium during municipal solid waste incineration. *J. Mater. Cycles Waste* **2016**, *18*, 287–295. [[CrossRef](#)]



© 2019 by the authors. Licensee MDPI, Basel, Switzerland. This article is an open access article distributed under the terms and conditions of the Creative Commons Attribution (CC BY) license (<http://creativecommons.org/licenses/by/4.0/>).